

Quadruply Differenced One-Way Ranging: QDOR

Gabor Lanyi*

ABSTRACT. — In the technique described in this article, the differential angular position of a spacecraft with respect to another spacecraft is determined by a radio interferometric technique that is designated here as quadruply differenced one-way ranging (QDOR). This technique allows very accurate planetary navigation with respect to orbital satellites within the Deep Space Network resources. The arrival signal phases of a spacecraft are differenced between two receiving antennas and then the resultant phase difference is differenced against another spacecraft. The resultant differential phase delay is calibrated by a quasar. The cycle ambiguities in the phase are determined from group-delay measurements of differential delta differential one-way ranging (Δ DOR); the ambiguity resolution depends on reducing certain Δ DOR errors. The presented cycle ambiguity resolution technique can also be applied to phase referencing to a quasar instead of a spacecraft; however, its confidence level will depend on the quasar position error. An analysis of a data set provides formal errors at the picosecond delay level with a temporal position resolution of 5 min. This is equivalent to about 0.05 nrad *differential* angular coordinate error that is approximately 10 m at Mars.

I. Introduction

We previously described four practical methods of interferometric technique that may be used to determine angular spacecraft positions: *delta differential one-way ranging* (Δ DOR), *phase referencing*, *radio frequency synthesis*, and *Earth rotation synthesis* [1]. This list is expanded here, by reporting on a fifth method: *quadruply differenced one-way ranging* (QDOR). This name was coined as a natural extension of the Δ DOR acronym (also used as DDOR) that may be interpreted as *doubly differenced one-way ranging*.

The method of phase referencing was applied to angular spacecraft tracking in 2004 to the Mars Exploration Rover B (MER-B) spacecraft at the 1-nrad error level (10 ps) [2]. The quoted article gave a description of a radio interferometric application of the 45-baseline Very Long Baseline Array (VLBA) for determining spacecraft position in the quasar reference frame. Additional results on VLBA measurements on Cassini were also reported in [3]. Related to this project, differential positions between two *near* spacecraft were also evaluated at a much lower error level of 2 ps. Results for improving the Saturn ephemeris by tracking

* Tracking Systems and Applications Section.

The research described in this publication was carried out by the Jet Propulsion Laboratory, California Institute of Technology, under a contract with the National Aeronautics and Space Administration. © 2011 California Institute of Technology. U.S. Government sponsorship acknowledged.

the Cassini spacecraft with VLBA at the 1-nrad error level in the quasar reference frame were reported recently in [4]. Position tracking of the Phoenix lander relative to orbiter spacecraft near Mars (Mars Odyssey and Mars Reconnaissance Orbiter) by the VLBA again achieved the 2-ps (0.19-nrad) error level at entry from post-evaluation of Mars approach [5].

Consequently, the question arose: could the Deep Space Network (DSN), using only two baselines, perform at the same or better error level than the VLBA with phase referencing?¹ Fundamentally, this is not a new question. Feasibility of differential Δ DOR between two spacecraft at Mars was studied over two decades ago with a predicted performance of 5 and 1-nrad angular navigation error at 40 and 250 MHz group delay spacings, respectively [6]. Before the existence of the VLBA, Edwards [7] examined phase delay interferometry on 6- and 250-km baselines with 1.6 to 20 deg angular quasar separation. However, the 250-km results did not appear to be fully convincing and the DSN did not (nor does) possess medium-length baselines. Short baselines could not compete with intercontinental baselines for accuracy irrespective of the technique used. Note also that the phase cycle resolution was limited to well known strong and stable position sources.

With better a priori source positions, improved bandwidth, sampling rate and resulting higher signal-to-noise ratios and shorter integration times, the chances of phase-based delay interferometry on a single intercontinental baseline are improved. Consequently, phase-delay based interferometry on DSN intercontinental baselines on strong nearby natural sources was successfully explored on a limited data set.² However, unless we use some of the aforementioned techniques to aid the phase cycle resolution, determining the final phase cycle ambiguity can be forbidding on intercontinental baselines with insufficient a priori position and media delay information, and weak sources. One possibility is using Δ DOR for cycle ambiguity resolution. Here, we present a method of differential spacecraft tracking that can be used with only two baselines, in the presence of Δ DOR tracking, at a higher accuracy level than given by VLBA phase referencing.

II. Methodology

In Δ DOR, the received phase $\varphi(v)$ of spacecraft tone signals are tracked for at least two frequencies at two receiving sites denoted by A and B, and then a group delay formed from the site differenced phases $\Delta\varphi(v) = \varphi_A(v) - \varphi_B(v)$: $x_{\Delta\text{DOR-SC}} = (\Delta\varphi(v_2) - \Delta\varphi(v_1))/\Delta v_{21}$, where $\Delta v_{21} = v_2 - v_1$ is the group delay frequency. In addition, a distant natural radio source angularly nearby with a continuous spectrum, typically a quasar, is observed by the two sites, in bands centered at v_1 and v_2 , and a differential group delay $x_{\Delta\text{DOR-QSR}}$ is extracted by the very long baseline interferometry (VLBI) technique. The final product is in essence the difference between the spacecraft and quasar delays, $x_{\Delta\text{DOR}} = x_{\Delta\text{DOR-SC}} - x_{\Delta\text{DOR-QSR}}$, for determining the angular coordinates of the spacecraft with respect to the quasar. The final group delay consists of two components: the true geometric delay x_{true} and a combination of various spurious delays that we consider as the error of measurement.

¹ The average baseline length of the VLBA is about three times shorter than the intercontinental DSN baselines; thus, for the same delay error level, the VLBA accuracy is approximately three times lower [2].

² W. Majid, personal communication, 2010.

In QDOR, the arrival signal phases of two spacecraft are tracked the same way as in Δ DOR. Each of the spacecraft phases is differenced between the two receiving sites, but then the resultant phase-difference delays $\Delta\phi(\nu)/\nu$ are differenced among themselves at differing frequencies of the two spacecraft, ν and ν' : $x_{\text{QDOR-SC}} = (\Delta\phi(\nu)/\nu - \Delta\phi'(\nu')/\nu')$. The VLBI procedure is carried out for a quasar with observing frequencies enveloping the two spacecraft frequencies ν and ν' . The differential phase delays of the quasar $x_{\Delta\text{DOR-QSR}(\nu)}$ at the two spacecraft frequencies are differenced and this differential delay calibrates the spacecraft measurement by subtraction: $x_{\text{QDOR}} = x_{\text{QDOR-SC}} - (x_{\Delta\text{DOR-QSR}(\nu)} - x_{\Delta\text{DOR-QSR}(\nu')})$. An angularly magnified view of the observational geometry is displayed in Figure 1. The cycle ambiguities in the phase values are determined from the group-delay measurements of differential Δ DOR for the two spacecraft. The success of cycle ambiguity resolution necessitates the reduction of certain Δ DOR errors.³ A statistical evaluation of a set of differential Δ DOR group delays sets the confidence level of cycle ambiguity resolution. Performing this procedure on two baselines determines the two differential angular coordinates. Due to delay measurements derived from phase and the absence of quasar coordinate uncertainty, QDOR provides substantially more accurate differential angular coordinate values with respect to a planet than the group-delay-based Δ DOR.

In general, it is expected that the observation sequence would start with an approximately 15-min observation of a quasar with a strength of ≥ 1 Jy correlated flux density. It is to be followed by a 30-min sequence of alternating observations of the two spacecraft with a duration between 15 and 60 s for each spacecraft, and a repeat of the quasar observation.

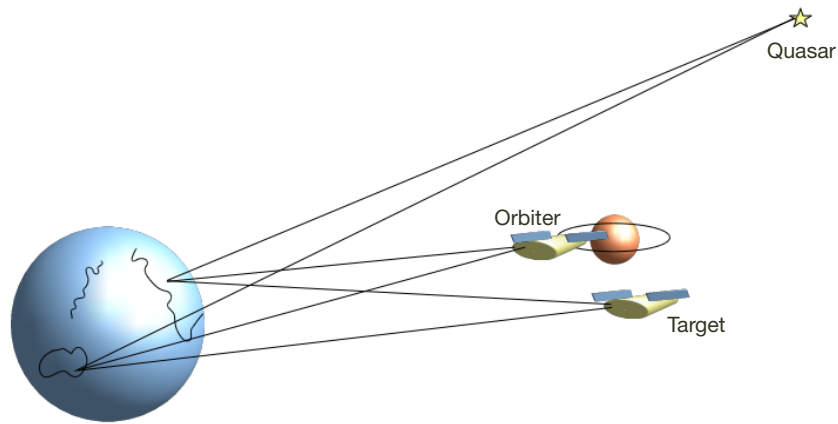


Figure 1. The geometry of delay-difference observations.

III. Data Analysis

During Δ DOR tracking of spacecraft, Mars Odyssey and Mars Reconnaissance Orbiter (MRO) were observed simultaneously within the beamwidth of two receiving antennas, DSS-26 and DSS-34, on November 6, 2010. As a part of the Δ DOR technique [8], a nearby quasar, P 1622-253, was also observed in a sequence alternating between the quasar and spacecraft. The observing frequencies were between 8.40 and 8.48 GHz (X-band), distributed among

³ Due to the absence of quasar position error and reduced media delays, the differential form of Δ DOR used here to resolve cycle ambiguities can be more accurate than ordinary Δ DOR if the instrumental phase ripple is reduced.

four 4-MHz observing bands for each spacecraft, with the largest separation of near 80 MHz. The data were recorded and reduced by phase tracking the spacecraft measurements, and by VLBI on the quasar. The obtained phase delays were referenced to spacecraft ephemeris tables provided by the Mars Odyssey and MRO flight projects⁴ and the a priori position of the quasar. The QDOR technique described in the previous section was applied to the residual phase delays after cycle-slip removal and the final result for one of the two closest frequency pairs, with about 5 MHz separation between the observing frequencies of the two spacecraft, is displayed in Figure 2.

A sinusoid function was statistically estimated from the spacecraft residual delays, since it appears that the residual delay represents the orbital correction due to its functional form and periodicity of about 2 hr. The anomalous first three values in the last spacecraft segment were excluded from the sinusoid fit. The amplitude of the sinusoid residual delay is 0.045 ± 0.003 X-band cycles with a standard deviation of 0.013 cycles around the sinusoid. The full residual scatter is the standard deviation of the sum of the sinusoid and its residual scatter: $\sqrt{0.045^2/2 + 0.013^2} = 0.034$ X-band cycles.⁵

To exhibit a correlation between the residual delays and orbital correction, a simple one-parameter correction to the orbital model was performed by shifting the time origin of the differential delay model, which corresponds to simultaneous rotation of both spacecraft. When the model was shifted by 7 milliseconds (ms) (about 6×10^{-6} rad of rotation), the sinusoid amplitude is decreased by a factor of two, as displayed in Figure 3.

In summary, the presented analysis provides evidence of formal errors at the picosecond delay level after removal of a small orbit correction, with a temporal position resolution of 5 min. This precision is equivalent to about 0.05 nrad differential angular coordinate error at the DSN that is approximately 10 m at Mars.

IV. Statistics of Cycle Ambiguity Resolution

The spacecraft ephemeris table used in data reduction is based on a large set of Doppler-shift measurements of the two orbital spacecraft with relatively short orbital periods. Therefore, one expects the functional form of differential residual phase delay to resemble the differential model delay and to possess an insignificant mean value over the orbital periods. Thus, something would need to be truly wrong to have a cycle offset (about a 1-km differential orbit error) between spacecraft delay points and the quasar line.

However, for spacecraft in cruise, wobbling spacecraft, partial orbital measurements, ephemerides with large uncertainties, or weak signals, one cannot rule out cycle offsets, and thus cycle ambiguities must be ascertained from differential Δ DOR measurements. This procedure will be described in this section.

Figure 2 shows an alternating sequence of differential phase delays of quasar and spacecraft. Originally, half of these delays were offset by one cycle with respect to each other. Figure 2

⁴ Orbit reconstructed ephemerides: spk_m_od39427-39507_rec_v1, spk_psp_rec20075_19982_20075_r-v1.

⁵ The integral of squared sinusoid equals to its peak-amplitude squared divided by 2.

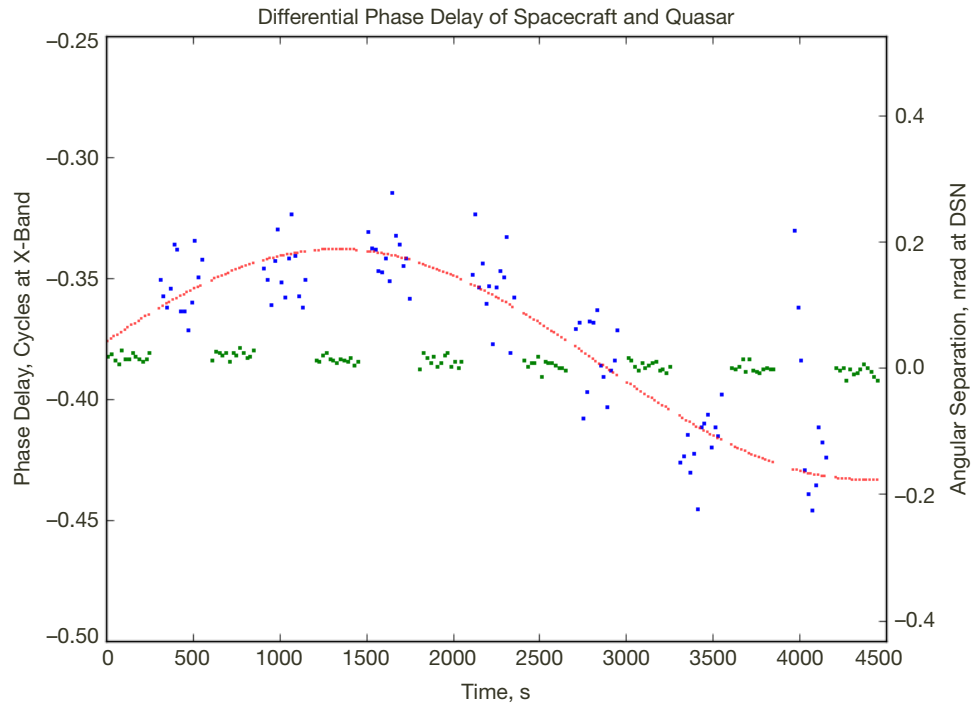


Figure 2. Displayed are the differential phase delay of spacecraft (blue sparse dots) and the the differential phase delay of the quasar (green dense dots). The differential position of the spacecraft is obtained by subtracting the differential quasar phase values. These position differences are denoted on the right-hand vertical axis of the figure. The sinusoid (red line) is a statistical fit to the spacecraft points.

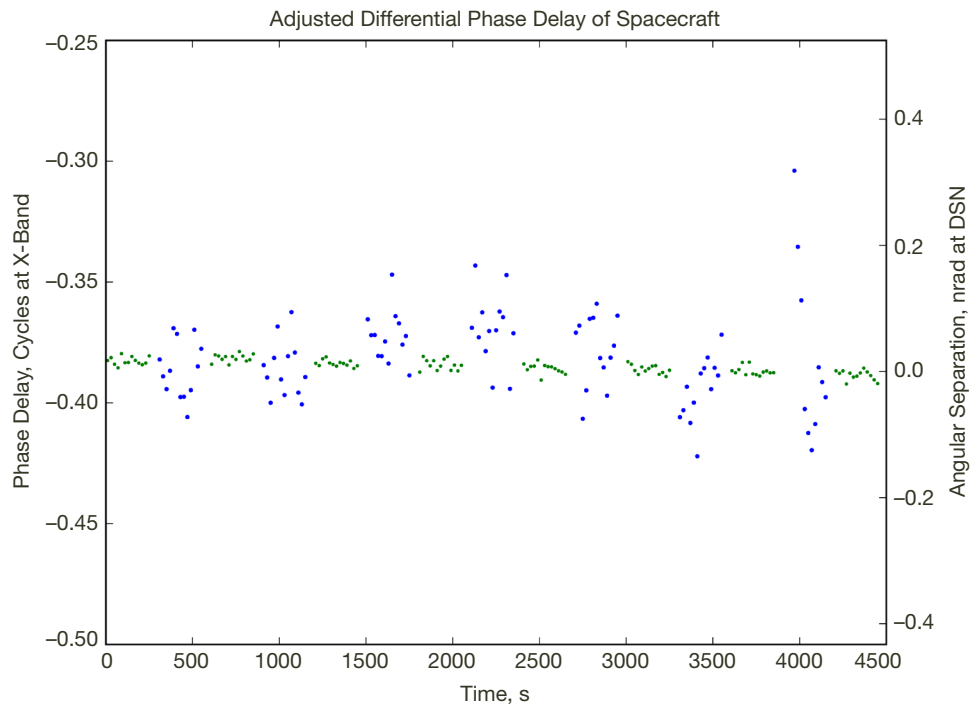


Figure 3. Same as Figure 2, except the temporal origin of the differential spacecraft model was shifted by 7 ms, corresponding to simultaneous rotation of both spacecraft by about 6×10^{-6} rad.

was obtained by moving all segments to the same baseline within one cycle. The result was checked against the differential Δ DOR delays and the result was a reasonable agreement. Well, what is a reasonable agreement?

In order to answer this question, one must first study the Δ DOR error budget. A version of the Δ DOR budget based on 40-MHz group delay considerations was published in [1] considering terrestrial and interplanetary media delays, station location, Earth orientation, thermal noise, clock error, and instrumental phase ripple. The error budget did not include the uncertainty of the quasar position. In the presented differential Δ DOR measurement, the quasar position error cancels, and all other contributions may be ignored but the thermal noise and instrumental phase ripple.

The average instrumental phase ripple magnitude, the deviation from a constant nominal value, was inferred indirectly from a large set of Δ DOR data. In the error budget of Δ DOR [1], the average magnitude of phase ripple was assumed to be 0.2 deg with an estimated ≈ 30 ps contribution to 40-MHz group delay measurements. This value is a bit above half of the maximum root-mean-squared (RMS) value of 0.35 deg obtained by a direct study [9] of a single Δ DOR experiment with 4-MHz band observations, which explores the calibration of the phase ripple. Note that the maximum value reported in the same study was 0.5 deg. Extrapolating the above information, this study assumes that the maximum magnitude of phase ripple is 0.6 deg, corresponding to 21 ps at each of the two frequency bands of an 80-MHz group delay observation ($0.6/360/80$ MHz = 21 ps ≈ 0.18 X-band cycle). With the same reasoning, 0.2 deg of phase ripple magnitude corresponds to 7 ps delay at each band.

The thermal noise is included in the standard deviation error of Δ DOR measurements. From the error budget of Δ DOR in [1], we obtain that the average thermal noise for differential Δ DOR for 80 MHz group delays involving two medium-gain spacecraft antennas is $\sigma_{total} = \sqrt{2} 19/2 \approx 14$ ps. At each of the four frequency bands of differential Δ DOR at 80 MHz group delay, this would correspond to $\sigma = 19\sqrt{2}/2 \approx 7$ ps. In this estimate of the thermal noise, the contribution of the quasar calibrator, with a strength of ≥ 1 Jy correlated flux density, is ignored.

If we now proceed according to the common simplistic view of data reduction statistics, then we have eight 7-ps Gaussian noise contributions for differential Δ DOR and the RMS value for a total standard deviation is $\sigma_{total} = 7\sqrt{8}$ ps = 20 ps. If we choose three standard deviations as the confidence interval, then we have that $3\sigma_{total} = 60$ ps, which is half of the X-band cycle; a satisfying result for cycle ambiguity resolution. However, the substantially more complex statistical consideration below indicates that the simplistic view above serves only as a guideline.

The instrumental phase ripple is assumed to be practically constant during an observation session. Therefore, the instrumental phase ripple will act like a bias in contrast to the Gaussian thermal noise, which randomly varies in an observing session and is thus estimable. However, we do not know the particular value of the bias β in a single experiment. For a large set of experiments with various observing frequencies, we assume that the probability distribution of phase ripple magnitude is constant ($1/2b_{max}$) between its maximum values $\pm b_{max}$.

The true value x_{true} is the actual geometric delay that is independent of the method of measurement. The measured differential ΔDOR delay value x is a sum of the true value x_{true} , the actual bias β , and the noise n , thus

$$x = x_{\text{true}} + \beta + n \quad (1)$$

The noise n randomly varies during an experiment and the bias β may have different values at different frequency bands and in other experiments. We need to limit that how far and how often β and n can move the measured differential ΔDOR delay x away from x_{true} within the \pm one cycle boundaries in a statistical sense. In the foregoing, we will limit the frequency of this motion by imposing limits on the statistical distribution of β and n . The standard deviation of noise is given by $\sigma = (\langle n^2 \rangle)^{1/2}$. We assume now that $|n| < 3\sigma$ with a Gaussian false probability of 2.8×10^{-3} and that $|\beta|$ is within the limits of a bias threshold b , where $b < b_{\text{max}}$ is chosen such that the probability $P(|\beta| > b) \approx 2.8 \times 10^{-3}$. Within these statistical limits, we can now examine how well differential ΔDOR can resolve a potential cycle offset in QDOR.

Due to the high precision of QDOR delay values compared to ΔDOR , we consider the true delay x_{true} as one of the x_{QDOR} delays lying on the QDOR cycle grid: the one that is being closest to the differential ΔDOR value x .⁶ If one needs to be very precise, then the QDOR delay error should also be considered in the statistics. Let us now assume that in Figure 2 the selected spacecraft delay segment values are potentially wrong by one cycle. The question is then the following: Could a particular measured differential ΔDOR delay x correspond to the case when the true delay x_{true} is at or beyond the one cycle boundaries? The answer is twofold:

- (1) *Half-cycle confidence test*: On the one hand, one should attempt to assure that the true value x_{true} is practically always on the right cycle by limiting the probability of false choice $P_{\text{false}} = P(|x - x_{\text{true}}| > \text{Half-cycle})$ to a small value. This is a sufficient but not a necessary condition. In general, we wish keep this probability in the neighborhood of 10^{-3} . Let us denote T_{half} as half of the full cycle T (120 ps at X-band). Considering the statistical limits we have set on the noise and bias right after Equation (1), the condition for the combined false choice probability $P(|x - x_{\text{true}}| > T_{\text{half}}) < 5.6 \times 10^{-3}$ for all measurements is equivalent, at this false choice level, to the inequality

$$3\sigma + b < T_{\text{half}} \quad (2)$$

- (2) *Full-cycle confidence test*: On the other hand, irrespective of whether the above half-cycle confidence test is satisfied, we can check a particular experimental value x against the adjacent full-cycle boundaries for potential cycle offset by the probability distribution of random noise and bias. For the given confidence level, this test of the absence of a false choice is a necessary condition. For an actual measured x value, this test of false choice checks whether the above probability limits for n and β are satisfied with respect to the adjacent cycle boundaries:

⁶ The cycle grid consists of the sequence $x_{\text{true}} + mT$, where m is an integer and T is the cycle interval.

$$T - |x - x_{true}| > 3\sigma + b =$$

$$T - |x_{diff-\Delta DOR} - x_{QDOR}| > 3\sigma + b \quad (3)$$

If Equation(3) is satisfied, then the choice is valid within the limit of the confidence level. The later *full-cycle confidence test* of the absence of a false choice, based on the combination of actual measurements and the inequality in Equation (3), is displayed in Figure 4. The differential measurement points, $x - x_{true} = x_{diff-\Delta DOR} - x_{QDOR}$, are shown as a function of the group delay frequency, in such a way that the differential ΔDOR group delays x with their measured 3σ standard deviation values varies and the assumed threshold value of bias b is fixed to the one-cycle boundaries: $|x - x_{true}| + 3\sigma < T - b$. The weighted average of delays is displayed on the right in this figure; the averaging process will be described below in the next section. With the given probability of false choice value of 5.6×10^{-3} , the edge of the error bar of the averaged delay should stay within the bias threshold boundaries, while the delay point by definition should also stay within the half-cycle boundaries.

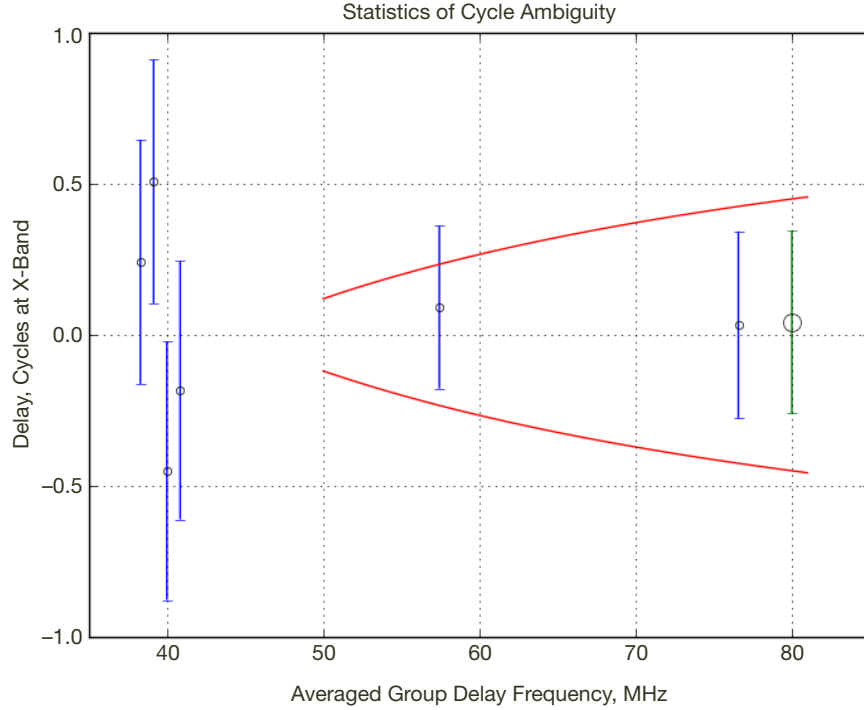


Figure 4. Full-cycle confidence test: statistical evaluation of differential ΔDOR group delays for a potential offset of one phase-cycle in QDOR. The horizontal axis represents the group-delay frequencies. The 6 individual points with 3σ error bars (blue) represent the differential ΔDOR delays $x - x_{true} = x_{diff-\Delta DOR} - x_{QDOR}$ formed from two ΔDOR delays with the same group delay frequency, relative to x_{QDOR} . The solid (red) line represents the bias limit $T - b$ at the 2.8×10^{-3} confidence level. This bias is the phase ripple deviation from the nominal value across the various 4-MHz observing bands. The (green) point with the big circle on the right represents the weighted average referenced to 80 MHz. Note that, while none of the delay errors satisfy the half-cycle confidence test of the absence of false choice at the 5.6×10^{-3} confidence level ($3\sigma + b < T_{half}$), the full-cycle confidence test of the best or averaged delay itself assures the absence of false choice at the same confidence level with a margin ($|x - x_{true}| + 3\sigma < T - b$).

We are now ready to check our simplistic guideline calculation of the confidence limit of QDOR for the presence of a cycle slip by the inequality of the half-cycle confidence test $3\sigma + b < T_{half}$, as applies to the above values of σ and b at 80 MHz with a combined confidence level of 5.6×10^{-3} . Using that $b = 0.389 \times 8 b_{max}$ for differential Δ DOR bias at the confidence level of 2.8×10^{-3} in Table 1, we obtain for the average delay case that $3\sigma + b = 3 \times 2\sigma + 3.1 b_{max} = 6 \times 7 \text{ ps} + 3.1 \times 21 \text{ ps} = 107 \text{ ps} > 60 \text{ ps} = T_{half}$. Therefore, our chosen confidence level is not satisfied and it can be shown from Table 1 and Gaussian probability values that the half-cycle false choice confidence is only at the 2×10^{-1} level, and it will be somewhat lower for low-gain transmitters and with the larger media-effects at larger angular separations. If we can reduce the maximum instrumental phase-ripple magnitude below 0.2 deg, then our chosen 5.6×10^{-3} confidence level will hold.

Table 1. Selected values of $P(\beta > b) = P(|\beta| > b)/2$ as the function of the fractional bias threshold. These are integrated probabilities of convoluted homogeneous bias distributions for frequency sequences of (0, 20, 40, 80). For single Δ DOR, $P(\beta > b) = 1/2(1 - b/b_{sum})^2$.

Probability of false choice (half-values)	Threshold fraction b/b_{sum}			
	Differential Δ DOR		Δ DOR	
	Single	Average of 6	Single	Average of 6
	$4\beta: b_{sum} = 4b_{max}$	$8\beta: b_{sum} = 8b_{max}$	$2\beta: b_{sum} = 2b_{max}$	$4\beta: b_{sum} = 4b_{max}$
0.7×10^{-3}	0.776	0.408	0.962	0.521
1.4×10^{-3}	0.786	0.389	0.948	0.503
2.8×10^{-3}	0.746	0.367	0.926	0.482
5.6×10^{-3}	0.697	0.338	0.896	0.455
11.2×10^{-3}	0.642	0.310	0.853	0.426
22.4×10^{-3}	0.573	0.277	0.791	0.385
44.8×10^{-3}	0.493	0.238	0.701	0.338
89.6×10^{-3}	0.394	0.191	0.579	0.275

Table 1 contains the probability of false choice $P(\beta_{avg} > b)$ as the function of the bias threshold ratio to the maximum bias for positive β_{avg} . Here, the probability $P(\beta_{avg} > b) = P(|\beta_{avg}| > b)/2$ is evaluated as a function of the threshold b . As was explained earlier, we assume that the probability distribution of the bias β is assumed to be homogeneous; a constant between $-b_{max}$ and b_{max} and zero otherwise. The probability distribution of β_{avg} is an eightfold convolution of the homogenous distribution function for the 8-variable case. It can be evaluated analytically; it consists of 8 patched segments of eight-order polynomials. The tail integral of this distribution function is displayed in Table 1 for a few values of b for differential and ordinary Δ DOR average and single delay values.

V. Statistical Averaging of Differential Δ DOR Delays

In this section we will attempt to reduce the errors of the differential Δ DOR delay $x_{diff-\Delta DOR}$ by narrowing the effective probability distribution of the noise n and the bias β via averaging over the delay values of differential Δ DOR at various group delay frequencies. For the current Δ DOR, the averaging can be done in two ways — average the Δ DOR delays first and then difference it between spacecraft, or difference first and then average. We will present

an averaging calculation that is independent of the averaging order. The averaging will result in no significant improvement compared to the single delay with the highest group delay frequency; nevertheless, the exercise is instructive and delay averaging can improve the success of the full-cycle confidence test.

By modifying slightly the current algorithm of Δ DOR, a third way of averaging is possible by estimating an average Δ DOR group delay as a gradient of phase against all different frequency bands and then calculating a single differential Δ DOR delay. Estimating an average Δ DOR delay as a gradient of phase will result in a bit better, but not a truly significant, improvement.

We will use four Δ DOR frequency bands in the description of averaging method, but our consideration is the same for any number of bands. Referenced to the lowest frequency band, there are two logical choices of frequency sequences of current Δ DOR when including the carrier frequency, in MHz: (0, 40, 60, 80) or (0, 20, 40, 80). The corresponding group delay frequencies $\Delta\nu$ are in MHz: (20, 40, 60, 80). The group delay is inverse proportional to the group delay frequency, and so thus the noise and the phase ripple bias. Therefore, to achieve uniform averaging, we will use weighted averaging of the Δ DOR delays by scaling these sources of errors to their 80-MHz group-delay frequency level by a factor of $\lambda = \Delta\nu/80$. Thus, the values of λ , in growing frequency order, are (0.25, 0.5, 0.75, 1.0).

There are $4 \times (4-1)/2 =$ six distinguishable Δ DOR group delays for four bands (half-off-diagonal part of the corresponding asymmetric 4×4 matrix), but only four independent variables for noise n and phase ripple bias b . The four indices 1 to 4 will be used singly for the band-dependent bias and noise, and in pairs for Δ DOR group delay related quantities, which involve two frequencies. In the following, the indices will run in increasing frequency order. According to Equation (1) with interpreting x_{true} as the Δ DOR geometric delay, and the definition of the Δ DOR delay $x_{\Delta\text{DOR-SC}}$ described in Section II, we select a Δ DOR group delay between band 2 and 1:

$$x_{21} = (\Delta\varphi(\nu_2) - \Delta\varphi(\nu_1))/\Delta\nu_{21} = x_{\text{true}} + \beta_{21} + n_{21} \quad (4)$$

where, if we denote the single-band noise and bias contribution to phase by $\Delta\varphi_n(\nu)$ and $\Delta\varphi_\beta(\nu)$, respectively, then $\beta_{21} + n_{21}$ can be written in four single-band components as⁷

$$\beta_{21} + n_{21} = \Delta\varphi_\beta(\nu_2)/\Delta\nu_{21} - \Delta\varphi_\beta(\nu_1)/\Delta\nu_{21} + \Delta\varphi_n(\nu_2)/\Delta\nu_{21} - \Delta\varphi_n(\nu_1)/\Delta\nu_{21} \quad (5)$$

Let us now mark the delay of the second spacecraft by the prime symbol x' . From the pairs of Δ DOR delays of two spacecraft (x, x') , we can then form a 6×6 matrix consisting of 36 differential Δ DOR group delays involving eight independent variables of n and b . However, in the following consideration, only six delays will be used, the diagonal part of the 6×6 differential Δ DOR delay matrix, which is shown in Table 2.⁸ This way, the weighted averaging method is equally applicable to ordinary Δ DOR and the exposition of the calculation is

⁷ All known information about bias and noise refers to differential, interferometric phase values between the two site receivers. Therefore, in our current consideration, the bias and the noise are not broken into site-dependent components in $\Delta\varphi$.

⁸ It can be shown that scaling and averaging over *all* the 36 differential delays reduces to the presented averaging of only the diagonal part of the 6×6 differential Δ DOR delay matrix.

Table 2. Pairing of 6 Δ DOR delays for two spacecraft. Pairs with the same group delay frequency are marked by the cross (\times) symbol. The left outer column and the top row represent the Δ DOR delays with indices in growing frequency band order, for the frequency series of (0, 20, 40, 80). The right outer column and the bottom row represent the group delay frequency in MHz.

	x_{21}	x_{32}	x_{31}	x_{43}	x_{42}	x_{41}	
x'_{21}	\times	\times					20
x'_{32}	\times	\times					20
x'_{31}			\times	\times			40
x'_{43}			\times	\times			40
x'_{42}					\times		60
x'_{41}						\times	80
	20	20	40	40	60	80	

simplified. We assume in the following that both spacecraft have the same band sequence, thus the index order is the same. The mixed case is similar, but the necessary pairing of the Δ DOR delays with the same group frequencies causes index remapping for one of the spacecraft.

If we now define the quantities $\bar{\beta}$ and \bar{n} as the 80-MHz group-delay-frequency representation of the bias and noise for indices 1 to 4, e.g., $\bar{\beta} = \lambda_{21} \Delta\varphi_{\beta}(v_2) / \Delta v_{21} = \Delta\varphi_{\beta}(v_2) / 80$, then the multiplication of Equation (5) by the scale factor λ_{21} and forming the difference for differential Δ DOR leads to Equation (6), since we matched the group delay frequencies of the two spacecraft and therefore $\lambda' = \lambda$ for all indices:

$$\begin{aligned} \lambda_{21}(x_{21} - x'_{21}) &= \lambda_{21}x_{\text{true}} + \lambda_{21}(\beta_{21} + n_{21} - (\beta'_{21} + n'_{21})) \\ &= \lambda_{21}x_{\text{true}} + \bar{\beta}_2 - \bar{\beta}_1 + \bar{n}_2 - \bar{n}_1 - (\bar{\beta}'_2 - \bar{\beta}'_1 + \bar{n}'_2 - \bar{n}'_1) \end{aligned} \quad (6)$$

where x_{true} is now the geometric delay of differential Δ DOR, and the double-indexed group frequency dependence vanished for the bias and noise. Applying Equation (6) to all six Δ DOR group delay terms will lead to sequences formed from the terms on the right-hand side of Equation (6) for both bias and noise as, e.g., $\bar{n}_4 - \bar{n}_1$, $\bar{n}_4 - \bar{n}_2$, $\bar{n}_4 - \bar{n}_3$, $\bar{n}_3 - \bar{n}_1$, $\bar{n}_3 - \bar{n}_2$, $\bar{n}_2 - \bar{n}_1$.

We are now ready to evaluate the average delay. If we denote the differential sum of all random variables by ε_i (i runs 1 to 4) and the sum of all λ values by λ_{sum} , and x_{avg} as the sum of the left-hand side of Equation (5) divided by λ_{sum} , then the weighted average of differential Δ DOR reduces to

$$\varepsilon_i = \bar{n}_1 + \bar{\beta}_i - \bar{n}'_i - \bar{\beta}'_i \quad (7)$$

$$\lambda_{\text{sum}} = \lambda_{41} + \lambda_{42} + \lambda_{43} + \lambda_{31} + \lambda_{32} + \lambda_{21} \quad (8)$$

$$x_{\text{avg}} = x_{\text{true}} + (1/\lambda_{\text{sum}})[(\varepsilon_4 - \varepsilon_1) + (\varepsilon_4 - \varepsilon_2) + (\varepsilon_4 - \varepsilon_3) + (\varepsilon_3 - \varepsilon_1) + (\varepsilon_3 - \varepsilon_2) + (\varepsilon_2 - \varepsilon_1)] \quad (9)$$

and thus the error terms are

$$x_{\text{avg}} - x_{\text{true}} = (1/\lambda_{\text{sum}})(3\mathcal{E}_4 + \mathcal{E}_3 - \mathcal{E}_2 - 3\mathcal{E}_1) \quad (10)$$

We evaluate now the needed λ values for the selected six Δ DOR group delays. For the observing band sequence (0, 20, 40, 80), the λ values are: $\lambda_{41} = 1.0$, $\lambda_{42} = 0.75$, $\lambda_{43} = 0.5$, $\lambda_{31} = 0.5$, $\lambda_{32} = 0.25$, $\lambda_{21} = 0.25$. For the other sequence, (0, 40, 60, 80), the λ values are: $\lambda_{41} = 1.0$, $\lambda_{42} = 0.5$, $\lambda_{43} = 0.25$, $\lambda_{31} = 0.75$, $\lambda_{32} = 0.25$, $\lambda_{21} = 0.5$. For both sequences, $\lambda_{\text{sum}} = 3.25$.

In general, the noise level $\sigma = (\langle n^2 \rangle)^{1/2}$ can be different for each of the four frequency bands, and thus if Equation (10) applied for noise only to evaluate the standard deviation $\langle \sigma \rangle$ of $x_{\text{avg}} - x_{\text{true}}$ by the RMS of all random independent terms of noise in Equation (10), we get that

$$\langle \sigma \rangle = (9\sigma_4^2 + \sigma_3^2 + \sigma_2^2 + 9\sigma_1^2)^{-1/2} / \lambda_{\text{sum}} \quad (11)$$

where, for all four indices

$$\sigma_i^2 = \langle n_i^2 \rangle + \langle n_i'^2 \rangle \quad (12)$$

The improvement factor with respect to a single 80-MHz differential Δ DOR delay is obtained by dividing $\langle \sigma \rangle$ with the corresponding single 80-MHz delay standard deviation of $(\langle n_4^2 \rangle + \langle n_4'^2 \rangle + \langle n_1^2 \rangle + \langle n_1'^2 \rangle)^{-1/2}$. As an approximation, substituting the same value for all standard deviations, we obtain that the average $\langle \sigma \rangle$ is $(\sqrt{20}/3.25)\sqrt{2}/2 = 0.98$ times the single 80-MHz differential Δ DOR value. For ordinary Δ DOR, the reduction factor is the same.

For the improvement factor of the bias with respect to a single 80-MHz differential Δ DOR, we need to consult the false choice probability for the differential Δ DOR bias threshold in Table 1. From this table, we obtain that $b = 0.389 \times 8 b_{\text{max}}$ at the confidence level of $2 \times 1.4 \times 10^{-3} = 2.8 \times 10^{-3}$ for the averaged delay and $b = 0.786 \times 4 b_{\text{max}}$ for the single 80-MHz differential Δ DOR delay. Thus, the improvement factor for the bias is $2 \times 0.389/0.786 = 0.99$. For ordinary Δ DOR, there is no reduction at high confidence levels. Thus, an averaging of differential or ordinary Δ DOR delays results in no significant improvement.

As the final step of this section, we formulate the phase gradient method of averaging and evaluate it for the frequency sequence $\nu = (0, 20, 40, 80)$ of both spacecraft. Since the lowest frequency ν_1 is defined as zero, the frequency ν will serve also as the group delay frequency referenced to ν_1 . For convenience, we will use same dimensionless scale factor defined above as applied to ν , $\lambda_i = \nu_i/\nu_4 = \nu_i/80$ for all four frequencies, and scale the differential phases into delays referenced to 80 MHz, $\eta = \Delta\varphi(\nu)/80$. This way, the formulation conforms the notation of this section and x_{avg} will transparently reduce to the ordinary Δ DOR group delay for the frequency pair (0, 80).

This averaging method models the phase $\Delta\varphi(\nu)$ (as η) as a linear function of the frequency ν (as λ) expressed now in the normalized variables as

$$\eta = \eta_1 + x_{\text{avg}} \lambda \quad (13)$$

and estimate the initial phase η_1 and the gradient-delay x_{avg} by minimizing the following sum of residual-squares of the measurements with weights w_i with respect to η_1 and x_{avg} :

$$\sum w_i (\eta_1 + x_{\text{avg}} \lambda_i - \eta_i)^2 \quad (14)$$

The above mathematical procedure is called linear regression, and its solution involves five quantities of scalar sums (S_0, S_1, S_2, Y_0, Y_1) of the vector components of the weights w_i , the values of independent variable λ , and the measurements η_i , and in addition the determinant D of the resultant two linear equations:

$$S_0 = \sum w_i \quad (15)$$

$$S_1 = \sum w_i \lambda_i \quad (16)$$

$$S_2 = \sum w_i \lambda_i^2 \quad (17)$$

$$Y_0 = \sum w_i \eta_i \quad (18)$$

$$Y_1 = \sum w_i \lambda_i \eta_i \quad (19)$$

$$D = S_0 S_2 - S_1^2 \quad (20)$$

with the solution

$$x_{\text{avg}} = (1/D)(S_0 Y_1 - S_1 Y_0) \quad (21)$$

$$\eta_1 = (1/D)(S_2 Y_0 - S_1 Y_1) \quad (22)$$

If we apply Equation (1) to the normalized differential Δ DOR variables as $\eta = x_{\text{true}} + \bar{\beta} + \bar{n}$ and denote the differential sum of all error variables, as in Equation (7), by $\varepsilon_i = \bar{\beta}_i + \bar{n}_i - (\bar{\beta}'_i + \bar{n}'_i)$, then the x_{avg} error terms from Equation (21), which correspond to Equation (10), are now

$$x_{\text{avg}} - x_{\text{true}} = (1/D)(S_0 \sum w_i \lambda_i \varepsilon_i - S_1 \sum w_i \varepsilon_i) \quad (23)$$

Applying equal weights of one to Equation (23), and denoting the number of frequency bands as $N = 4$, we obtain that

$$x_{\text{avg}} - x_{\text{true}} \left(\sum \lambda_i^2 - N^{-1} (\sum \lambda_i)^2 \right)^{-1} \sum (\lambda_i - N^{-1} \sum_k \lambda_k) \varepsilon_i \quad (24)$$

As an approximation, setting all standard deviations of noise to $\sigma = \langle n^2 \rangle$, the average standard deviation of noise for differential Δ DOR by the RMS of Equation (24) is then

$$\langle \sigma \rangle = \sqrt{2} \sigma (D/N)^{-1/2} = \sqrt{2} \sigma \left(\sum \lambda_i^2 - N^{-1} (\sum \lambda_i)^2 \right)^{-1/2} \quad (25)$$

In our case, $N = 4$, $\sum \lambda_i = \lambda_{\text{sum}} = 1 + 1/2 + 1/4 = 1.75$, $\sum \lambda_i^2 = \lambda_{\text{sum}}^2 = 1 + (1/2)^2 + (1/4)^2 = 1.31$, thus the improvement with respect to the single differential Δ DOR group delay of 2σ is $(1.31 - 1.75^2/4)^{-1/2} \sqrt{2} \sigma / 2\sigma = (2 \times (1.31 - 1.75^2/4))^{-1/2} = 0.96$, not a truly significant improvement. For the confidence level of 2.8×10^{-3} , the bias improvement is similar. Note that the improvement of the group delay error would be better with an optimally designed frequency sequence.

VI. Conclusion

The presented method of differential position determination between two spacecraft appears to be a solid procedure with high precision for small angular separations. Media-induced delay effects will degrade its precision with larger angular separations, but not substantially within 0.1 deg of spacecraft separation, which is equivalent to about 30 days out for Mars approach. In general, one needs to observe alternately the two spacecraft and the quasar with antenna movement, adding temporal to the spatial effects of media delay. The ruggedness of the technique relies on solid Δ DOR measurements for phase cycle ambiguity resolution; the current half-cycle false choice confidence is estimated to be only at the 0.2 level (equivalent to 1.3- σ Gaussian noise) if the overall magnitude of instrumental phase ripple does not exceed 0.6 deg. Instrumental phase ripple for Δ DOR had to be seriously considered and any reduction of its magnitude is strongly desirable to make the cycle ambiguity resolution more rugged, that is, in particular needed for larger angular separations or low-gain transmitters. Using the calibration technique described in [9], the QDOR quasar may be applied for phase ripple reduction; otherwise, an appropriate high-strength quasar observation after the normal observation sequence should be performed. Additionally, an effort to calibrate or reduce the instrumental phase ripple at its origin would be equally appropriate. In its current state, Δ DOR could not calibrate the cycle ambiguities at 32 GHz (Ka-band). For this case, the group delay frequency would need to be increased by fourfold.

Acknowledgments

The Δ DOR processed data set used for the analysis in this report was kindly provided by James Border. The comments of J. Border and C. Naudet are also much appreciated.

References

- [1] G. Lanyi, D. S. Bagri, and J. S. Border, "Angular Position Determination of Spacecraft by Radio Interferometry," *Proceedings of the IEEE*, vol. 95, pp. 2193–2201, November 2007.
- [2] G. Lanyi, J. Border, J. Benson, V. Dhawan, E. Fomalont, T. Martín-Mur, T. McElrath, J. Romney, and C. Walker, "Determination of Angular Separation between Spacecraft and Quasars with the Very Long Baseline Array," *The Interplanetary Network Progress Report*, vol. 42-162, Jet Propulsion Laboratory, Pasadena, California, pp. 1–16, August 15, 2005. http://ipnpr.jpl.nasa.gov/progress_report/42-162/162A.pdf
- [3] T. Martín-Mur, P. Antreasian, J. Border, J. Benson, V. Dhawan, E. Fomalont, E. Graat, R. Jacobson, G. Lanyi, T. McElrath, J. Romney, and C. Walker, "Use of Very Long Baseline Array Interferometric Data for Spacecraft Navigation," International Symposium on Space Technology and Science, STS 2006-d-50, 2006. <http://archive.ists.or.jp>
- [4] D. L. Jones, E. Fomalont, V. Dhawan, J. Romney, W. M. Folkner, G. Lanyi, J. Border, and R. A. Jacobson, "Very Long Baseline Array Astrometric Observations of the Cassini Spacecraft at Saturn," *Astronomical Journal*, vol. 141, no. 2, article 29, pp. 1–10, 2011.

- [5] T. J. Martín-Mur and D. E. Highsmith, "Mars Approach Navigation Using the VLBA," 21st International Symposium on Space Flight Dynamics, Toulouse, France, 2009. [http://www.mediatec-dif.com/issfd/Orbitdl/Martin Mur.pdf](http://www.mediatec-dif.com/issfd/Orbitdl/Martin%20Mur.pdf)
- [6] C. D. Edwards, "Short Baseline Phase Delay Interferometry," *The Telecommunications and Data Acquisition Progress Report*, vol. 42-91, Jet Propulsion Laboratory, Pasadena, California, pp. 46–56, July–September 1987. http://ipnpr.jpl.nasa.gov/progress_report/42-91/91D.PDF
- [7] C. D. Edwards, W. M. Folkner, J. S. Border, and L. J. Wood, "Spacecraft–Spacecraft Very Long Baseline Interferometry for Planetary Approach Navigation," *Proceedings of the 1st AAS/AIAA Annual Spaceflight Mechanics Meeting*, Houston, Texas, A93-17901 05-13, pp. 1161–1181, 1991.
- [8] C. L. Thornton and J. S. Border, "Radiometric Tracking Techniques for Deep Space Navigation," *JPL Deep Space Communications and Navigation Series*, J. H. Yuen, ed., New Jersey: John Wiley & Sons, Inc., 2003.
- [9] S. T. Lowe, "A Measurement of X-Band Front-End Phase Dispersion for Delta-Differenced One-Way Range (DDOR) Experiments," *The Interplanetary Network Progress Report*, vol. 42-184, Jet Propulsion Laboratory, Pasadena, California, pp. 1–15, February 15, 2011. http://ipnpr.jpl.nasa.gov/progress_report/42-184/184B.pdf